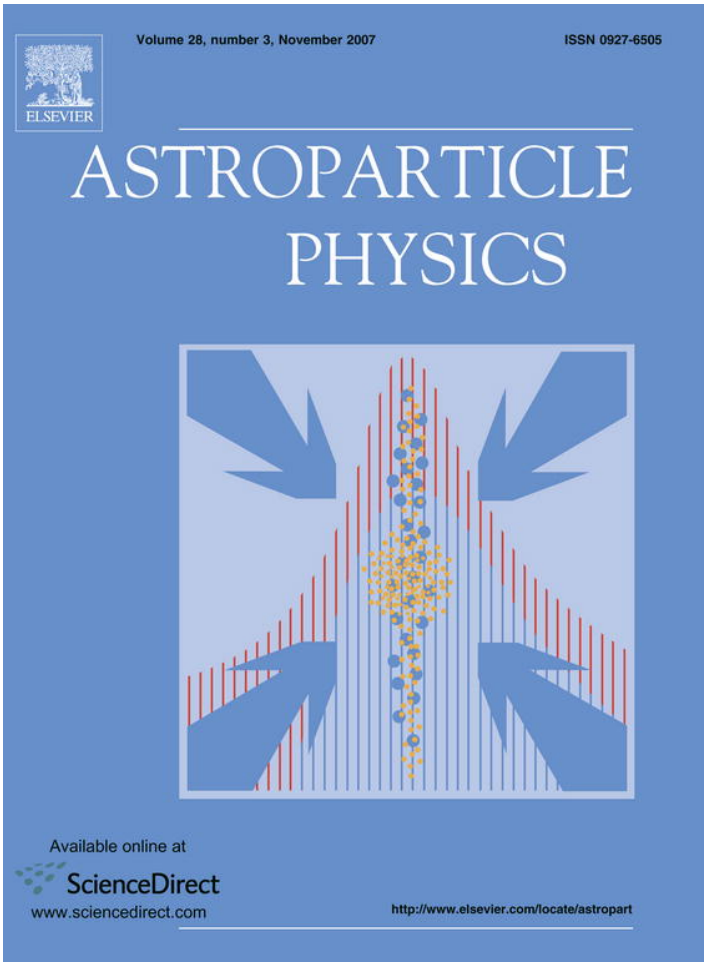

Available online at www.sciencedirect.com
ScienceDirect
Astroparticle Physics 28 (2007) 321–326
Astroparticle Physics
www.elsevier.com/locate/astropart

Mutually compensative pseudo solutions of primary energy spectra in the knee region

S.V. Ter-Antonyan *

Yerevan Physics Institute, Department of Cosmic Ray Physics, 2 Alikhanyan Brothers Street, 375036 Yerevan, Armenia

Received 31 August 2006; received in revised form 6 June 2007; accepted 23 June 2007
Available online 28 June 2007

Abstract

The problem of the uniqueness of solutions during the evaluation of primary energy spectra in the knee region using an extensive air shower (EAS) data set and the EAS inverse approach is investigated. It is shown that the unfolding of primary energy spectra in the knee region leads to mutually compensative pseudo solutions. These solutions may be the reason for the observed disagreements in the elementary energy spectra of cosmic rays in the 1–100 PeV energy range obtained from different experiments.

PACS: 96.40.Pq; 96.40.De; 96.40.−z; 98.70.Sa

Keywords: Cosmic rays; Primary energy spectra; Extensive air shower; Inverse problem

1. Introduction

The extensive air shower (EAS) inverse approach to a problem of the primary energy spectra reconstruction in the region of 1–100 PeV energies has been an essential tool in the past decade [1–7]. Basically, it follows from the high accuracies of recent experiments [8–12] and the availability of the EAS simulation code [13], which was developed in the framework of contemporary interaction models in order to compute the kernel functions of a corresponding integral equation set [6,11]. At the same time, the energy spectra of primary (H, He and Fe) nuclei obtained from the KASCADE experiment [6] using the EAS inverse approach disagree with the same data from the ongoing GAMMA experiment [11,12], where parameterization of the EAS inverse problem is used.

Below, a peculiarity of the EAS inverse problem is investigated, and one of the possible reasons for the observed disagreements between the energy spectra in [6] and [11] is considered in the framework of the SIBYLL [14] interaction model.

The paper is organized as follows. In Section 2 the EAS inverse approach and the definition of the problem of uniqueness is described. It is shown, that the abundance of primary nuclear species leads to pseudo solutions for unfolded primary energy spectra. The existence and significance of the pseudo solutions are shown in Section 4. The pseudo solutions for primary energy spectra were obtained on the basis of simulation of KASCADE [6] shower spectra. The EAS simulation model is presented in Section 3. In Section 5 the peculiarities of the pseudo solutions are discussed in comparison with the methodical errors of the KASCADE data.

2. Problem of uniqueness

The EAS inverse problem is ill-posed by definition and the unfolding of the corresponding integral equations does not ensure the uniqueness of the solutions. The regularized unfolding on the basis of *a priori* information on expected

* Tel.: +374 10 250374.
E-mail address: samvel@yerphi.am

0927-6505/$ - see front matter © 2007 Elsevier B.V. All rights reserved.
doi:10.1016/j.astropartphys.2007.06.004

solutions (smoothness, monotony and non-negativity) in some cases can redefine the inverse problem [15] and provide the appropriate solutions. However, the expected singularities (e.g., knees) in the primary energy spectra at 10^{15}–10^{16} eV may erroneously be smoothed by regularization algorithms and vice versa, be imitated by the unavoidable oscillations [15] of the solutions. Furthermore, the EAS inverse problem implies evaluations of at least two or more unknown primary energy spectra from the integral equation set of Fredholm kind [6,11,12]. These peculiarities have not been studied in detail and the problem of the uniqueness of solutions can limit the number of evaluated spectra.

Let $f_A(E)$ be the energy spectrum of a primary nucleus A over the atmosphere, $W_A(\mathbf{x}|E)$ be the probability density function describing the transformation of A and E parameters of the primary nucleus to a measurable vector $\mathbf{x}$. Then the EAS inverse problem, i.e., the reconstruction of the energy spectra of N_A primary nuclei on the basis of the detected spectra $Y(\mathbf{x})$ of EAS parameters, is defined by the integral equation

$$Y(\mathbf{x}) = \sum_{A=A_1}^{A_{N_A}} \int f_A(E) W_A(\mathbf{x}|E) \mathrm{d}E. \tag{1}$$

Evidently, if $f_{A_1,\ldots A_{N_A}}(E)$ are the solutions of Eq. (1), the functions $f_A(E) + g_A(E)$ should also be the solutions of (1), provided equation

$$\sum_A \int g_A(E) W_A(\mathbf{x}|E) \mathrm{d}E = 0(\pm\Delta Y), \tag{2}$$

is satisfied for the given measurement errors $\Delta Y(\mathbf{x})$ and for at least one of the combinations of the primary nuclei

$$n_C = \sum_{j=1}^{N_A} \binom{N_A}{j}. \tag{3}$$

The number of combinations (3) stems from a possibility of the existence of a set of functions $g_A(E) \equiv g_{1,A}(E), \ldots, g_{i,A}(E)$ for each of the primary nuclei (A), which can independently satisfy Eq. (2).

For example, suppose that $N_A = 3$. Let us denote $\int g_{i,A_k}(E) W_{A_k}(E)\mathrm{d}E$ by I_{i,A_k} and, for simplicity, set the right-hand side of Eq. (2) to 0. Then, following expression (3), we find $n_C = 7$ independent combinations of Eq. (2): $I_{1,A_k} = 0$ for $k = 1$, 2, and 3, $I_{2,A_1} + I_{2,A_2} = 0$, $I_{3,A_1} + I_{2,A_3} = 0$, $I_{3,A_2} + I_{3,A_3} = 0$ and $I_{4,A_1} + I_{4,A_2} + I_{4,A_3} = 0$ with different $g_{i,A_k}(E)$ functions. The measurement errors $\pm\Delta Y$ on the right-hand side of these equations can both increase and decrease the domains of $g_{i,A_k}(E)$ functions.

One may call the set of functions $g_A(E)$ the pseudo functions with the corresponding pseudo solutions (spectra) $f_A(E) + g_A(E)$. The oscillating $g_A(E) \equiv g_{1,A}(E)$ functions at $j = 1$ are responsible for the first N_A equations $\int g_{1,A}(E) W_A(\mathbf{x}|E)\mathrm{d}E = 0(\pm\Delta Y)$, $A \equiv A_1, \ldots A_{N_A}$, due to the positive-definite probability density function $W_A(E)$. The pseudo solutions $f_A(E) + g_{1,A}(E)$ can be avoided by using iterative unfolding algorithms [6,15].

Additional sources of the pseudo solutions originate from the mutually compensative effects at $j \geqslant 2$:

$$-\sum_k \int g_{A_k}(E) W_{A_k}(\mathbf{x}|E)\mathrm{d}E \simeq \sum_{m\neq k} \int g_{A_m}(E) W_{A_m}(\mathbf{x}|E)\mathrm{d}E, \tag{4}$$

inherent to Eq. (2) for arbitrary groups of k and $m \neq k$ primary nuclei. Since there are no limitations on the types of the pseudo functions (except for $f_A(E) + g_A(E) > 0$) that would follow from expression (4), and the number of possible combinations (3) rapidly increases with the number of evaluated primary spectra (N_A), the problem of the uniqueness of solutions may be insoluble for $N_A > 3$. Moreover, the pseudo functions have to restrict the efficiency of unfolding energy spectra for $N_A \simeq 2$–3, because the unification of $Z = 1, \ldots, 28$ primary nuclei spectra into 2–3 nuclear species (e.g., light and heavy) inevitably increases the uncertainties of the kernel functions $W_A(E)$ and thereby also increases the domains of the pseudo functions.

Notice, that the pseudo solutions will always appear in the iterative unfolding algorithms if the initial iterative values are varied within large intervals. At the same time, it is practically impossible to derive the pseudo functions from the unfolding of Eqs. (1) and (2) due to a strong ill-posedness of the inverse problem. However, for a given set of the measurement errors $\Delta Y(\mathbf{x})$ and the known kernel functions $W_A(\mathbf{x}|E)$ for $A \equiv A_1, \ldots A_{N_A}$ primary nuclei, Eq. (2) can be regularized by parametrization of the pseudo functions $g_A(\alpha, \beta, \ldots|E)$. The unknown parameters $(\alpha, \beta, \ldots)$ can be derived from a numerical solution of parametric Eq. (2), and thereby one may also evaluate the parametrized pseudo functions $g_A(E)$.

Below (Section 3), an EAS simulation model for computing the kernel function $W_A(E)$ and replicating the KASCADE [6] EAS spectral errors $\Delta Y(\mathbf{x})$ is considered.

3. EAS simulation model

The primary energy spectra obtained in the KASCADE experiment were derived on the basis of the detected 2-dimensional EAS size spectra $Y(\mathbf{x}) \equiv Y(N_e, N_\mu)$ and an iterative unfolding algorithm [15] for $N_A = 5$ primary nuclei [6]. Evidently, whether these solutions are unique or not depends on the significance of the arbitrary pseudo functions $|g_A(E)|$ from Eq. (2).

We suppose that the convolution of the shower spectra $W_A(N_e, N_\mu|E)$ at the observation level and corresponding measurement errors $\sigma(N_e), \sigma(N_\mu)$ [1] are described by 2-dimensional log-normal distributions with parameters $\xi_e = \overline{\ln N_e}(A,E), \xi_\mu = \overline{\ln N_\mu}(A,E), \sigma_e(A,E), \sigma_\mu(A,E)$ and correlation coefficients $\rho_{e,\mu}(A,E)$ between the shower size ($\ln N_e$) and the muon truncated size ($\ln N_\mu$). We tested this hypothesis by the χ^2 goodness-of-fit test using the CORS-

IKA(NKG) EAS simulation code [13] for the SIBYLL2.1 [14] interaction model, 4 kinds of primary nuclei ($A \equiv$ p, He, O, Fe), 5 energies ($E \equiv 1$, 3.16, 10, 31.6, 100 PeV) and simulation samples for each of E and A: 5000, 3000, 2000, 1500, 1000, respectively in 0–18° zenith angular interval. The values of corresponding $\chi^2(A_i, E_j)/n_{\text{d.f.}}, (i = 1, \ldots 4, j = 1, \ldots 5)$ were distributed randomly in the interval 0.5–1.4 for the measurement ranges of the KASCADE experiment ($N_{e,\min} = 6.3 \times 10^4$ and $N_{\mu,\min} = 4 \times 10^3$) and the bin sizes $\Delta \ln N_e, \Delta \ln N_\mu = 0.075$.

Notice, that the combined 2-dimensional log-normal distributions with parameters $\sigma_{e,1}(A,E)$ at $\ln N_e < \xi_e$, $\sigma_{e,2}(A,E)$ at $\ln N_e > \xi_e, \sigma_{\mu,1}(A,E)$ at $\ln N_\mu < \xi_\mu$ and $\sigma_{\mu,2}(A,E)$ at $\ln N_\mu > \xi_\mu$, more precisely ($\chi^2/n_{d.f.} \leqslant 1.2$) describe the shower spectra $W_A(N_e, N_\mu|E)$ in the tail regions.

We performed an additional test of the log-normal fit of the W_A spectra using multiple correlation analysis for the shower parameters simulated by the log-normal $W_A(N_e, N_\mu|E)$ probability density functions and shower parameters obtained from the CORSIKA EAS simulations at power-law primary energy spectra ($\gamma = -1.5$) and equivalent abundances of primary nuclei. The corresponding correlation coefficients were equal to $\rho(\ln E|\ln N_e, \ln N_\mu) = 0.97, \rho(\ln A|\ln N_e, \ln N_\mu) = 0.71$, $\rho(\ln A, \ln N_e) = -0.14 \pm 0.01$, $\rho(\ln A, \ln N_\mu) = 0.18 \pm 0.01$, and were in close agreement for both methods of N_e and N_μ generations.

We replicated the KASCADE 2-dimensional EAS size spectrum $Y(N_e, N_\mu)$ (and corresponding ΔY) by picking out N_e and N_μ randomly from the 2-dimensional shower spectra $W_A(N_e, N_\mu|E)$ after randomly picking A and E parameters of a primary particle from the power-law energy spectra

$$f_A(E) \propto E^{-2.7}\left(1 + \left(\frac{E}{E_k}\right)^{\epsilon}\right)^{-0.5/\epsilon}, \tag{5}$$

with a rigidity-dependent knee $E_k = Z \times 2000TV$, the sharpness parameter $\epsilon = 3$ and normalization of the all-particle spectrum $\int \sum_A f_A(E)\mathrm{d}E = 1$. The relative abundance of nuclei was arbitrarily chosen to be 0.3, 0.45, 0.15 and 0.1 for primary H, He, O and Fe nuclei respectively, which approximately conforms with the expected abundance from balloon and satellite data [16]. The mediate values of the parameters of the probability density function $W_A(N_e, N_m|E)$ were estimated by the corresponding log-parabolic splines.

The total number of simulated EAS events was set to 7×10^5 in order to replicate the corresponding statistical errors $\Delta Y(N_e, N_\mu)$ of the KASCADE data.

4. Pseudo solutions

On the basis of the obtained estimations of $\Delta Y(N_e, N_\mu)$ (Section 3) for the KASCADE experiment, we examined the uniqueness of unfolding (1) by χ^2-the minimization:

$$\chi^2 = \sum_{i=1}^{I}\sum_{j=1}^{J}\left(\frac{G(N_{e,i}, N_{\mu,j})}{\Delta Y(N_{e,i}, N_{\mu,j})}\right)^2, \tag{6}$$

where $G(N_{e,i}, N_{\mu,j})$ represents the left-hand side of Eq. (2) for 2 kinds of the empirical pseudo functions:

$$g_A(E) = \alpha_A\left(\frac{E}{E_m}\right)^{-\gamma_A}, \tag{7}$$

$$g_A(E) = \alpha_A((\ln E - \beta_A)^3 + \eta_A)\left(\frac{E}{E_m}\right)^{-3}, \tag{8}$$

while $g_A(E) + f_A(E) > 0$, otherwise $g_A(E) = -f_A(E)$. The unknown $\alpha_A, \beta_A, \gamma_A$ and η_A parameters in expressions (7) and (8) were derived from χ^2 minimization (6). The numbers of bins were $I = 60$ and $J = 45$ with the bin size $\Delta \ln N_e$, $\Delta \ln N_\mu \simeq 0.1$.

In fact, the minimization of χ^2 (6) for different representations (7) and (8) of the pseudo functions $g_A(E)$ provides a solution of the corresponding parametric Eq. (2) with a zero right-hand side. To avoid the trivial solutions $g_A(E) \equiv 0$ and reveal the domains of the pseudo functions, the values of some of the parameters were arbitrarily fixed during the minimization of χ^2 (6). The magnitudes of the fixed parameters were empirically determined via optimization of conditions $\chi^2_{\min}/n_{\text{d.f.}} \simeq 1$ and $|g_A(E)| \sim f_A(E)$ for the pseudo spectra with the fixed parameters.

The true primary energy spectra $f_A(E)$ for $A \equiv$ H, He, O, Fe nuclei (5) and the all-particle energy spectrum $\sum f_A(E)$ (lines) along with the corresponding distorted (pseudo) spectra $f_A(E) + g_A(E)$ (symbols) are presented in Fig. 1 respectively. The parameters of the pseudo functions (7) derived for $\chi^2_{\min}/n_{\text{d.f.}} = 1.08 (n_{\text{d.f.}} = 717)$ are presented in Table 1.

The effect of the pseudo functions (8) on the resulting primary energy spectra is shown in Fig. 2. Evaluations of the corresponding parameters are presented in Table 2 for $\chi^2_{\min}/n_{\text{d.f.}} = 1.1$. The variations of the cubic power

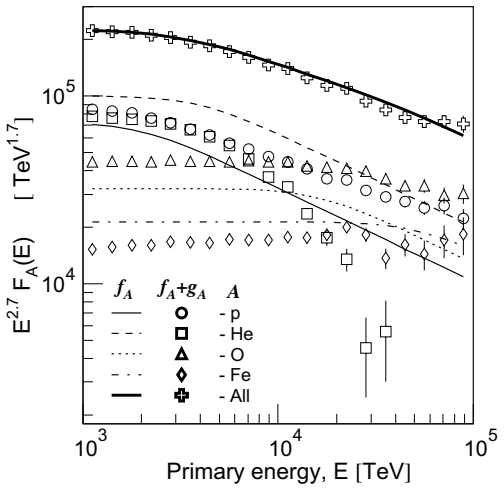

Fig. 1. Primary energy spectra $f_A(E)$ and the all-particle spectrum $\sum f_A(E)$ for $A \equiv$ H, He, O, Fe nuclei (lines) and the corresponding pseudo solutions $f_A(E) + g_A(E)$ for the pseudo function (7) (symbols).

Table 1
Parameters α_A (TeV^{-1}) and γ_A of the pseudo function (7) for different primary nuclei A and $E_m = 1000$ TeV

A	$\alpha_A \times 10^4$	γ_A
p	1.10 ± 0.06	2.71 ± 0.04
He	-1.80 (fixed)	2.60 (fixed)
O	0.97 ± 0.05	2.65 ± 0.04
Fe	-0.50 (fixed)	2.90 (fixed)

Table 2
Parameters α_A (TeV^{-1}), γ_A and η of the pseudo function (8) for different primary nuclei A and $E_m = 1000$ TeV

A	$\alpha_A \times 10^4$	β_A	η_A
p	-9.00 (fixed)	7.76 ± 0.01	0 (fixed)
He	0.044 ± 0.02	13.2 ± 1.08	169 ± 98
O	-0.80 (fixed)	8.47 ± 0.05	0.94 ± 0.16
Fe	0.010 ± 0.002	11.4 ± 0.14	50 (fixed)

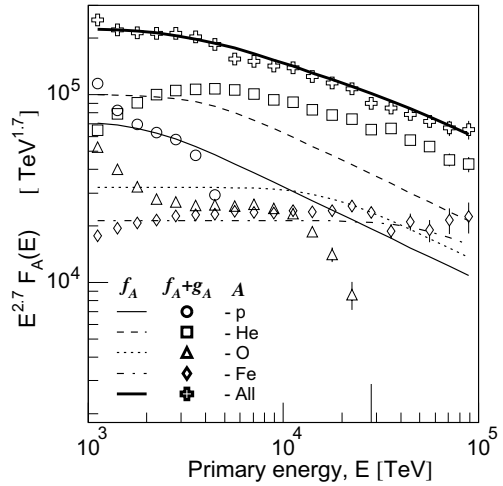

Fig. 2. The same as Fig. 1 for the pseudo function (8).

indices in expression (8) in the range of $2-5$ lead to different types of pseudo solutions as well.

It is clear from Figs. 1 and 2, that the contribution of the pseudo functions $g_A(E)$ can be comparable and even significantly larger than the values of the true spectra $f_A(E)$. Moreover, the pseudo solutions lose both the slopes and the intensities of the spectra. At the same time, the all-particle spectra slightly depend on the contribution of the pseudo functions.

The same results (Tables 1 and 2) were obtained using both the combined 2-dimensional log-normal representation of the shower spectra $W_A(N_e, N_\mu|E)$ (Section 3) and the 3-dimensional $(\ln E, \ln N_e, \ln N_\mu)$ parabolic interpolations of corresponding probability density functions obtained by the CORSIKA code.

Evidently, the range of relatively large measurement errors $\Delta Y(\mathbf{x})$ expands the domain of the pseudo functions. Contributions of the mutually compensative effects (Eqs. (2) and (4)) of the pseudo functions to the domain of the pseudo solutions were tested using a 10 times larger EAS simulation sample ($n = 7 \times 10^6$) and the pseudo functions with evident singularity:

$$g_A(E) = \alpha_A \varepsilon_A^{-1} \left(\frac{E}{\varepsilon_A}\right)^{\delta}, \tag{9}$$

where $\delta = -1$ at $E \leqslant \varepsilon_A$ and $\delta = -7$ at $E > \varepsilon_A$. The singularity of the pseudo function (9) for $A \equiv H$ was fixed at $\varepsilon_H = 3000$ TeV and the scale factor $\alpha_H = -0.03$. The remaining parameters for primary nuclei $A \equiv$ He, O, Fe were estimated by χ^2-minimization (6) and presented in Table 3 for $\chi^2_{\min}/n_{\text{d.f.}} = 2.01$ and $n_{\text{d.f.}} = 857$. The accuracies of integrations (2) were about 0.1%. The corresponding pseudo solutions are shown in Fig. 3.

Since the measurement errors are negligibly small, the significance of the mutually compensative effects is well seen. The singularity of the proton spectrum was approximately compensated by the He and O spectra. This is due to both the large number ($n_C = 15$) of possible mutually compensative combinations (3) and the peculiarities of EAS development in the atmosphere (kernel functions $W_A(E)$, Section 3), which are expressed by the approximately log–linear dependences of the statistical parameters $\langle \ln N_e \rangle, \langle \ln N_\mu \rangle, \sigma_e$ and σ_μ of shower spectra $W_A(E)$ on energy $(\ln E)$ and nucleon number $(\ln A)$ of primary nuclei [20,21]. The value of $\chi^2_{\min}/n_{\text{d.f.}}$ for a 10 times smaller EAS sample ($n = 7 \times 10^5$) was equal to 0.25.

Table 3
Parameters α_A (TeV^{-1}) and ε_A (TeV) of the pseudo function (9) for different primary nuclei A and $\varepsilon_H = 3000$ TeV

A	$\alpha_A \times 100$	$\varepsilon_A/\varepsilon_H$
p	-3.0 (fixed)	1 (fixed)
He	3.05 ± 0.07	1.03 ± 0.01
O	-0.84 ± 0.06	1.08 ± 0.03
Fe	0.15 ± 0.02	1.29 ± 0.10

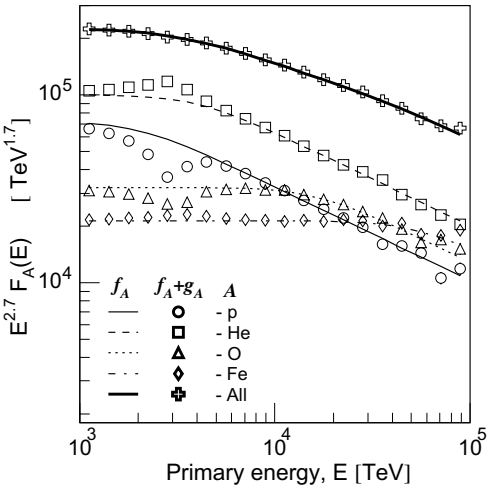

Fig. 3. The same as Fig. 1 for the pseudo function (9) and $n = 7 \times 10^6$ simulated showers.

5. Discussion

The results from Figs. 1–3 show that the pseudo functions with mutually compensative effects exist and belong practically to all families – linear (7), non-liner (8) and even singular (9) in a logarithmic scale.

The all-particle energy spectra in Figs. 1–3 are practically indifferent to the pseudo solutions of elemental spectra. This fact directly follows from Eq. (2) for pseudo solutions and is well confirmed by the identity of the GAMMA [11,12] and KASCADE [6] all-particle energy spectra in spite of disagreements of the elemental (p, He, Fe) primary energy spectra (see [11,12]).

The χ^2 minimization (6) uses mainly the nearest pseudo energy spectra with free parameters for compensation of the pseudo spectra with fixed parameters. The significance of the pseudo functions $|g_A(E)|$ in most cases exceeds the significance of the evaluated primary energy spectra $f_A(E)$ and unfolding of (1) can not be effective for $N_A = 4$.

The unfolding of the primary energy spectra for $N_A = 5$ will increase the number of possible combinations (3) of the pseudo solutions and the corresponding pseudo functions by a factor of two. Taking into account the large values of applied $\chi^2_{\min}/n_{\text{d.f.}} \simeq 2$–3 [6] one may conclude that the contributions of the pseudo functions in the unfolded energy spectra of [6] have to be dominant.

The "methodical errors" obtained in [6] for $N_A = 5$ define the uncertainties of the solutions intrinsic only to the given unfolding algorithms. The existence and significance of the mutually compensative pseudo solutions follow from Eqs. (1) and (2) and from the peculiarities of the shower spectra $W_A(\mathbf{x}|E)$ regardless of the unfolding algorithms.

Comparison of the methodical errors $(f_A(E)+\Delta f_A(E))/f_A(E)$ for $A \equiv$ He and $A \equiv$ Fe from [6] with corresponding errors $(f_A(E) + g_A(E))/f_A(E)$ due to the pseudo solutions from expressions (7) and (8) are shown in Fig. 4. The magnitudes of the fixed parameters were empirically determined by maximizing $|g_{\text{He}}(E)|$ (left panel) and $|g_{\text{Fe}}(E)|$ (right panel) for a given goodness-of-fit test $\chi^2_{\min}/n_{\text{d.f.}} \simeq 2.5$ from [6].

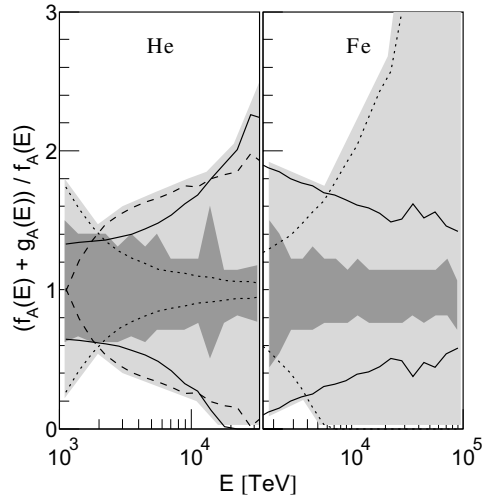

Fig. 4. Domains of the pseudo solutions for He and Fe primary nuclei (light shaded areas) and corresponding "methodical errors" of the KASCADE unfolding spectra (dark shaded areas) taken from [6]. The solid and dotted lines resulted from pseudo functions (7) and the dashed lines stemmed from (8).

It is seen that the methodical errors (dark shaded areas) from [6] significantly underestimate the contribution of the pseudo solutions (light shaded areas) from expressions (7) and (8). Moreover, the methodical errors from [6] slightly depend on the primary energy (or statistical errors), whereas the domains of the pseudo solutions strongly correlate with the statistical errors according to definition (2).

6. Conclusion

The results show that the reconstruction of primary energy spectra using unfolding algorithms [6,15] can not be effective and the disagreement between the KASCADE [6] and GAMMA [11,12] data is insignificant in comparison with the large domains of the mutually compensative pseudo solutions (Fig. 4) of the unfolded spectra [6].

Even though the oscillating pseudo solutions $g_{1,A}(E)$ (Section 2) are possible to avoid using regularization algorithms [15], the mutually compensative effect (4) of the arbitrary pseudo functions $g_A(E)$ intrinsic to the expression (2) is practically impossible to avoid at $N_A > 1$.

The uncertainties of solutions due to the mutually compensative pseudo functions can be obtained by varying the initial values of iterations within a wide range in the frameworks of a given unfolding algorithm.

To decrease the contributions of the mutually compensative pseudo solutions one may apply a parameterization of the integral Eq. (1) [1,2,4,11,12] using *a priori* (expected from theories [17–19]) known primary energy spectra with a set of free spectral parameters. This transforms the EAS inverse problem into a set of equations with unknown spectral parameters, and thereby the EAS inverse problem is transmuted into a test of the given primary energy spectra using detected EAS data [4]. The reliability of the solutions can be determined by their stability depending on the number of spectral parameters, the agreement between the expected and detected EAS data sets, and the conformity of the spectral parameters with theoretic predictions.

The all-particle energy spectra (Figs. 1–3) are practically indifferent toward the pseudo solutions for elemental spectra.

The obtained results depend slightly on the spectral representations of the shower spectra $W_A(E)$ and the primary energy spectra $f_A(E)$.

Acknowledgements

I thank my colleagues from the GAMMA experiment for stimulating this work and the anonymous referee for suggestions which considerably improved the paper.

References

[1] R. Glasstetter et al., in: Proc. 26th ICRC, Salt Lake City, 1 (1999) 222.
[2] S.V. Ter-Antonyan, L.S. Haroyan (2000), hep-ex/0003006.
[3] H. Ulrich et al., in: Proc. 27th ICRC, Hamburg, 1 (2001) 97.
[4] S.V. Ter-Antonyan, P.L. Biermann, in: Proc. 27th ICRC, Hamburg, HE054 (2001) 1051, astro-ph/0106091.
[5] Samvel Ter-Antonyan, Peter Biermann, in: Proc. 28th ICRC, Tsukuba, HE1, (2003) 235, astro-ph/0302201.
[6] T. Antoni et al., Astropart. Phys. 24 (2005) 1. astro-ph/0505413.
[7] R.M. Martirosov et al., in: Proc. of 29th ICRC, Pune, HE1.5, 8 (2005) 9, astro-ph/0506588.
[8] M. Aglietta et al., Astropart. Phys. 10 (1999) 1.
[9] M.A.K. Glasmacher et al., Astropart. Phys. 10 (1999) 291.
[10] T. Antoni et al., Nucl. Instrum Meth. A 513 (2003) 490.
[11] S.V. Ter-Antonyan et al., in: Proc. of 29th ICRC, Pune, HE1.2, 6 (2005) 105, astro-ph/0506588.
[12] A.P. Garyka et al., Astropart. Phys., doi: 10.1016/j.astropartphys., 2007.04.004, arXiv:0704.3200v1 (astro-ph).
[13] D. Heck, J. Knapp, J.N. Capdevielle, G. Schatz, T. Thouw, Forschungszentrum Karlsruhe Report, FZKA 6019 (1998).
[14] R.S. Fletcher, T.K. Gaisser, P. Lipari, T. Stanev, Phys. Rev. D 50 (1994) 5710.
[15] R. Gold, ANL-6984 Report, Argonne (1964).
[16] B. Wiebel-Sooth, P.L. Bierman, H. Meyer, Astron. Astrophys. 330 (1998) 330.
[17] A.M. Hillas, J. Phys. G 31 (2005) R95.
[18] J.R. Hörandel, Astropart. Phys. 21 (2004) 241.
[19] T. Stanev, P.L. Biermann, T.K. Gaisser, Astron. Astrophys. 274 (1993) 902.
[20] S.V. Ter-Antonyan, in: Proc. of 28th ICRC, Tsukuba, HE2 (2003) 239, astro-ph/0303658.
[21] J.R.Hörandel, astro-ph/0611387 (2006).